Jestr

Journal of Engineering Science and Technology Review 17 (5) (2024) 87-93

Research Article

JOURNAL OF
Engineering Science and Technology Review

www.jestr.org

The Analytical Model for Elastic Deformation of Cement Sheath in Well Cementing

Yuanbo Xia[1,2], Xi Chen[3], Junhua Liu[4], Yantao Xu[5] and Chengwen Wang[1,*]

[1]*School of Petroleum Engineering, China University of Petroleum (East China), Qingdao 266580, China*
[2]*CNPC Tianjin Bo-Xing Engineering Science &Technology Co., Ltd., Tianjin 300451, China*
[3]*Underground Operation Company, Chuanqing Drilling Engineering Co., Ltd., Chengdu 610051, China*
[4]*Second Drilling Engineering Branch, Bohai Drilling Engineering Company, Langfang 065000, China*
[5]*China Oilfield Services Limited, Tianjin 300451, China*

Received 17 July 2024; Accepted 29 September 2024

Abstract

During oil and gas extraction, alternating wellbore pressures can induce cyclic loading, which can potentially lead to structural damage of the casing cement sheath, posing safety risks. An analytical model for the elastic deformation stage of the cement sheath was developed to investigate its mechanical response and failure modes during well operations. A casing-cement sheath-formation system model and thick-walled cylinder theory were utilized. Analytical expressions for the elastic deformation stage were derived. These expressions were validated through finite element analysis. Results show that, the cement sheath primarily fails in either tensile or compressive modes. As the elastic modulus increases, a transition from compressive to tensile failure modes occurs. When the elastic modulus exceeds 40 GPa, the effect on radial stress stabilizes. Moreover, when the casing pressure reaches 60 MPa, the cement sheath expands outward, transitioning from a compressive state to a tensile state in the circumferential direction. This study provides valuable insights for analysing mechanical response parameters and evaluating the safety of the casing cement sheath during operations.

Keywords: Cement sheath, Elastic deformation, Failure, Finite element method

1. Introduction

Cementing is crucial in oil and gas extraction, providing well stability and preventing formation gas and groundwater infiltration, thereby enhancing safety during operations. Cement slurry forming a cement sheath through hydration. This sheath isolates the formation and supports the casing.

With the rise of unconventional resources like shale gas, issues such as casing deformation from volumetric fracturing have become increasingly common. Such deformation can impede bridge plug setting, reduce fracturing stages, increase costs, and decrease production, affecting the economic viability of shale gas projects. Additionally, alternating stress during operations can cause micro-cracks or gaps in the cement sheath, compromising its sealing ability and reducing well lifespan.

Early studies on cement sheaths led to improved mechanical models and experimental methods, but field damage and failure persist [1-3]. The cement sheath's mechanical response is influenced by casing and formation deformation. Thus, addressing the deformation coordination and developing a rapid calculation method for analyzing the cement sheath's mechanical response during elastic deformation are crucial.

This study developed the model for elastic deformation. The model was tested against finite element numerical solutions. The influence of parameters on stress and displacement fields was checked by this model. This study aims to identify primary failure modes and evaluate parameter impacts under operational conditions. This study was vital for maintaining cement sheath integrity and optimizing resource development.

2. State of the art

Oil and gas resources are essential for energy development, making the study of cement sheaths in well cementing crucial. Advances in science and technology have heightened this focus. Shu et al. found that cyclic loading induces micro-cracks in cement sheaths, increasing permeability and potentially leading to through-cracks. Micro-annular gaps, due to damage accumulation, are a key reason for gas migration in well cementing. However, this study was limited to a single gas storage facility [4]. De et al. used finite element methods to analyze casing-cement sheath-formation models, and obtained a strong correlation between failure and the stiffness ratio during pressure tests. The impact of temperature differentials on cement sheath damage was significant in oil well operations, though real-world complexity limited the application [5]. Deng et al. included interface failure factors in models to assess the effects of parameters on casing stress, but their study didn't account for interface damage or elastic modulus degradation [6]. Zhang et al. introduced a method for determining cement sheath thickness variations using dual-energy window methods, which were validated only through simulation [7]. Guo et al. found that cyclic loading led to micro-annular gaps at the cement sheath interface, which could cause gas migration. They noted that latex and toughening agents improve sealing by filling gaps and reducing pore size, but their study only considered circular cement sheaths, which were rarely perfect in real scenarios [8]. Zhou et al. observed that cement sheaths in the plastic deformation stage faced "interface stress reversal" risks under alternating pressures, leading to sealing failure. This study was based on simulation without experimental

*E-mail address: wangcwupc1@126.com
ISSN: 1791-2377
doi:10.25103/jestr.175.12

validation [9]. Zhang et al. developed an elastoplastic correction solution using the Mohr-Coulomb yield criterion for casing-cement sheath-formation assemblies under uniform pressures. This solution was limited to formations with small differential stresses and uniform in-situ stresses [10]. Wang et al. found that poor cementing quality affected casing stress and deformation, with excessive micro-gaps amplifying internal pressure effects. However, their work was specific to certain wells and has limited broader applicability [11]. Ghavami et al. used geological mechanics and finite element methods to propose a new design equation for predicting casing collapse, with constraints to improve accuracy. This method was specific to a southern Iran oil field and lacked detailed validation [12].

In addition to studying overall aspects of oil wells, scholars explored various methods to improve efficiency. Ugarte et al. found that hydrogen molecules enhance the formation of silicates and ettringite, which alter porosity distribution and improve cement strength. However, this study did not consider temperature and pressure changes, highlighting the need for further work to include these variables for an improved simulation of underground conditions [13]. Salim et al. emphasized the effective cementing for oil production, particularly the use of spacer fluids for pre-cementing cleaning. However, their experiments, conducted under controlled laboratory conditions, cannot fully represent the complexities of field oil well operations [14]. Nanomaterials recently attracted attention for their potential to optimize cement sheath properties and reduce strength degradation; however, their high cost renders them economically unfeasible for direct application in the oil industry [15]. Ahmed et al. indicated that delamination is more likely to occur at the cement-liner interface. The risk was highest in production liners, followed by shallow liners, with intermediate liners being the least susceptible to failure. Stress evaluation was crucial, particularly at elevated temperatures [16]. Furthermore, machine learning technologies were increasingly applied in cementing and oil fields. Support vector machines could predict the condition of cement sheaths in oil wells with the accuracy rate higher than 0.99 and the time consumption did not exceed one millisecond. Nonetheless, the reliance on training data from simulated cases of cement sheath damage necessitated a comprehensive database to achieve accurate predictions.

Existing studies primarily addressed finite element simulations and experimental studies of cement sheath deformation in specific wells. However, these studies were confined to particular wells and did not extensively investigate the impact of parameters on the cement sheath. Consequently, current findings exhibit limited applicability and cannot be generalized. Therefore, there is an urgent need for a rapid evaluation model to assess the mechanical response and failure under field conditions. This study proposes an analytical model of cement sheath during elastic deformation, and validates it through finite element methods. The study examines how factors affect its stress and displacement fields. This model is intended for evaluating the mechanical response and failure across various casing-cement sheath-formation configurations, providing a foundation for rapid and safe field evaluations.

The remainder of this study is organized as follows. Section 3 presents the mechanical and finite element models, along with the theoretical derivation of the analytical model. Section 4 validates the analytical model and explores the influence of different factors on the internal conditions. The final section summarizes the findings and presents conclusions.

3. Methodology

3.1 Mechanical model

Based on the theory of multi-layer thick-walled cylinders in elasticity, the combination of casing, cement sheath, and formation are modeled as a thick-walled cylinder comprising three different isotropic materials. Consequently, the Lame solution in elasticity is used for the calculations. [17].

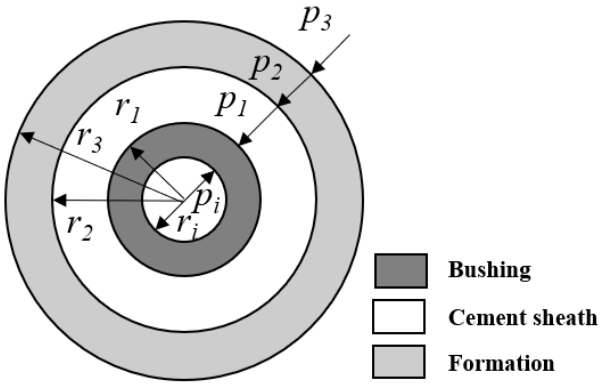

Fig. 1. Elastic mechanical model

The model is illustrated in Fig. 1. Expressions for radial stress and displacement can be derived using thick-walled cylinder theory, as detailed in equations (1) to (6).

Bushing：

$$\sigma_r^{ca\,\mathrm{sing}}=\frac{r_i^2}{r_1^2-r_i^2}\left(1-\frac{r_1^2}{r^2}\right)P_i-\frac{r_1^2}{r_1^2-r_i^2}\left(1-\frac{r_i^2}{r^2}\right)P_1 \tag{1}$$

$$u_r^{ca\,\mathrm{sing}}=\frac{\left(1+\nu_{ca\,\mathrm{sing}}\right)r}{E_{ca\,\mathrm{sing}}\left(r_1^2-r_i^2\right)}\left\{\left[\left(1-2\nu_{ca\,\mathrm{sing}}\right)r_i^2+\frac{r_i^2r_1^2}{r^2}\right]P_i-\left[\left(1-2\nu_{ca\,\mathrm{sing}}\right)r_1^2+\frac{r_i^2r_1^2}{r^2}\right]P_1\right\} \tag{2}$$

Cement sheath $(r_1\le r\le r_2)$：

$$\sigma_r^{cement}=\frac{r_1^2}{r_2^2-r_1^2}\left(1-\frac{r_2^2}{r^2}\right)P_1-\frac{r_2^2}{r_2^2-r_1^2}\left(1-\frac{r_1^2}{r^2}\right)P_2 \tag{3}$$

$$u_r^{cement}=\frac{\left(1+\nu_{cement}\right)r}{E_{cement}\left(r_2^2-r_1^2\right)}\left\{\left[\left(1-2\nu_{cement}\right)+\frac{r_2^2}{r^2}\right]r_1^2P_1-\left[\left(1-2\nu_{cement}\right)+\frac{r_1^2}{r^2}\right]r_2^2P_2\right\} \tag{4}$$

Formation $(r_2\le r\le r_3)$：

$$\sigma_r^{stratum}=\frac{r_2^2}{r_3^2-r_2^2}\left(1-\frac{r_3^2}{r^2}\right)P_2-\frac{r_3^2}{r_3^2-r_2^2}\left(1-\frac{r_2^2}{r^2}\right)P_3 \tag{5}$$

$$u_r^{stratum}=\frac{\left(1+\nu_{stratum}\right)r}{E_{stratum}\left(r_3^2-r_2^2\right)}\left\{\left[\left(1-2\nu_{stratum}\right)+\frac{r_3^2}{r^2}\right]r_2^2P_2-\left[\left(1-2\nu_{stratum}\right)+\frac{r_2^2}{r^2}\right]r_3^2P_3\right\} \tag{6}$$

In the formula: $\sigma_r^{ca\,\mathrm{sing}}$ is the radial stress of the casing, $u_r^{ca\,\mathrm{sing}}$ is the radial displacement of the casing, σ_r^{cement} is the radial stress of the cement sheath, u_r^{cement} is the radial displacement of the cement sheath, $\sigma_r^{stratum}$ is the radial stress

of the formation, and $u_r^{stratum}$ is the radial displacement of the formation ring.

3.2 Analytical model for cement sheath

According to the principle that the displacement of the outer interface must be consistent with the displacement at the inner boundary of the cement sheath, and the displacement at the outer interface must align with the displacement of the formation, the following equation can be obtained:

$$\begin{cases} u_{r=r_1}^{ca\sin g} = u_{r=r_1}^{cement} \\ u_{r=r_2}^{stratum} = u_{r=r_2}^{cement} \end{cases} \tag{7}$$

Substituting equations (3) and (6) into $r = r_1$, and substituting equations (6) and (9) into $r = r_2$, we can obtain expressions (8) to (15):

$$u_{r=r_1}^{ca\sin g} = \frac{(1+\nu_{ca\sin g})}{E_{ca\sin g}} \frac{2(1-\nu_{ca\sin g}) r_i^2 r_1}{r_1^2 - r_i^2} P_i - \frac{(1+\nu_{ca\sin g})}{E_{ca\sin g}} \frac{(1-2\nu_{ca\sin g}) r_1^3 + r_i^2 r_1}{r_1^2 - r_i^2} P_1 \tag{8}$$

$$u_{r=r_1}^{ca\sin g} = X_1^{ca\sin g} P_i - X_2^{ca\sin g} P_1 \tag{9}$$

$$u_{r=r_1}^{cement} = \frac{(1+\nu_{cement})}{E_{cement}} \frac{(1-2\nu_{cement}) r_1^3 + r_1 r_2^2}{r_2^2 - r_1^2} P_1 - \frac{(1+\nu_{cement})}{E_{cement}} \frac{2(1-\nu_{cement}) r_1 r_2^2}{r_2^2 - r_1^2} P_2 \tag{10}$$

$$u_{r=r_1}^{cement} = X_3^{cement} P_1 - X_4^{cement} P_2 \tag{11}$$

$$u_{r=r_2}^{cement} = \frac{(1+\nu_{cement})}{E_{cement}} \frac{2(1-\nu_{cement}) r_1^2 r_2}{r_2^2 - r_1^2} P_1 - \frac{(1+\nu_{cement})}{E_{cement}} \frac{(1-2\nu_{cement}) r_2^3 + r_1^2 r_2}{r_2^2 - r_1^2} P_2 \tag{12}$$

$$u_{r=r_2}^{cement} = X_5^{cement} P_1 - X_6^{cement} P_2 \tag{13}$$

$$u_{r=r_2}^{stratum} = \frac{(1+\nu_{stratum})}{E_{stratum}} \frac{(1-2\nu_{stratum}) r_2^3 + r_3^2 r_2}{r_3^2 - r_2^2} P_2 - \frac{(1+\nu_{stratum})}{E_{stratum}} \frac{2(1-\nu_{stratum}) r_3^2 r_2}{r_3^2 - r_2^2} P_3 \tag{14}$$

$$u_{r=r_2}^{stratum} = X_7^{stratum} P_2 - X_8^{stratum} P_3 \tag{15}$$

Among them:

$$X_1^{ca\sin g} = \frac{(1+\nu_{ca\sin g})}{E_{ca\sin g}} \frac{2(1-\nu_{ca\sin g}) r_i^2 r_1}{r_1^2 - r_i^2} \tag{16}$$

$$X_2^{ca\sin g} = \frac{(1+\nu_{ca\sin g})}{E_{ca\sin g}} \frac{(1-2\nu_{ca\sin g}) r_1^3 + r_i^2 r_1}{r_1^2 - r_i^2} \tag{17}$$

$$X_3^{cement} = \frac{(1+\nu_{cement})}{E_{cement}} \frac{(1-2\nu_{cement}) r_1^3 + r_2^2 r_1}{r_2^2 - r_1^2} \tag{18}$$

$$X_4^{cement} = \frac{(1+\nu_{cement})}{E_{cement}} \frac{2(1-\nu_{cement}) r_2^2 r_1}{r_2^2 - r_1^2} \tag{19}$$

$$X_5^{cement} = \frac{(1+\nu_{cement})}{E_{cement}} \frac{2(1-\nu_{cement}) r_1^2 r_2}{r_2^2 - r_1^2} \tag{20}$$

$$X_6^{cement} = \frac{(1+\nu_{cement})}{E_{cement}} \frac{(1-2\nu_{cement}) r_2^3 + r_1^2 r_2}{r_2^2 - r_1^2} \tag{21}$$

$$X_7^{stratum} = \frac{(1+\nu_{stratum})}{E_{stratum}} \frac{(1-2\nu_{stratum}) r_2^3 + r_3^2 r_2}{r_3^2 - r_2^2} \tag{22}$$

$$X_8^{stratum} = \frac{(1+\nu_{stratum})}{E_{stratum}} \frac{2(1-\nu_{stratum}) r_3^2 r_2}{r_3^2 - r_2^2} \tag{23}$$

Calculate the simplified expressions for P_1 and P_2, as shown in equations (24) and (25).

$$P_1 = \frac{X_1^{ca\sin g}\left(X_6^{cement} + X_7^{stratum}\right) P_i + X_4^{cement} X_8^{stratum} P_3}{\left(X_2^{ca\sin g} + X_3^{cement}\right)\left(X_6^{cement} + X_7^{stratum}\right) - X_4^{cement} X_5^{cement}} \tag{24}$$

$$P_2 = \frac{X_1^{ca\sin g} X_5^{cement} P_i + \left(X_2^{ca\sin g} + X_3^{cement}\right) X_8^{stratum} P_3}{\left(X_2^{ca\sin g} + X_3^{cement}\right)\left(X_6^{cement} + X_7^{stratum}\right) - X_4^{cement} X_5^{cement}} \tag{25}$$

By substituting P_1 and P_2 into equations (3) to (4), the expressions for the stress and displacement can be obtained:

$$\begin{aligned} \sigma_r^{cement} = {} & \frac{r_1^2}{r_2^2 - r_1^2}\left(1 - \frac{r_2^2}{r^2}\right) \frac{X_1^{ca\sin g}\left(X_6^{cement} + X_7^{stratum}\right) P_i + X_4^{cement} X_8^{stratum} P_3}{\left(X_2^{ca\sin g} + X_3^{cement}\right)\left(X_6^{cement} + X_7^{stratum}\right) - X_4^{cement} X_5^{cement}} \\ & - \frac{r_2^2}{r_2^2 - r_1^2}\left(1 - \frac{r_1^2}{r^2}\right) \frac{X_1^{ca\sin g} X_5^{cement} P_i + \left(X_2^{ca\sin g} + X_3^{cement}\right) X_8^{stratum} P_3}{\left(X_2^{ca\sin g} + X_3^{cement}\right)\left(X_6^{cement} + X_7^{stratum}\right) - X_4^{cement} X_5^{cement}} \end{aligned} \tag{26}$$

$$u_r^{cement} = \frac{(1+\nu_{cement}) r}{E_{cement}\left(r_2^2 - r_1^2\right)} \left\{ \begin{aligned} & \left[\left(1-2\nu_{cement}\right) + \frac{r_2^2}{r^2}\right] r_2^2 \frac{X_1^{ca\sin g}\left(X_6^{cement} + X_7^{stratum}\right) P_i + X_4^{cement} X_8^{stratum} P_3}{\left(X_2^{ca\sin g} + X_3^{cement}\right)\left(X_6^{cement} + X_7^{stratum}\right) - X_4^{cement} X_5^{cement}} \\ & - \left[\left(1-2\nu_{cement}\right) + \frac{r_1^2}{r^2}\right] r_2^2 \frac{X_1^{ca\sin g} X_5^{cement} P_i + \left(X_2^{ca\sin g} + X_3^{cement}\right) X_8^{stratum} P_3}{\left(X_2^{ca\sin g} + X_3^{cement}\right)\left(X_6^{cement} + X_7^{stratum}\right) - X_4^{cement} X_5^{cement}} \end{aligned} \right\} \tag{27}$$

Table 1. Material Mechanics Parameters

Material	Elastic modulus (GPa)	Density (kg/m^3)	Poisson's ratio
Stratum	6	1577	0.2
Cement ring	10	2500	0.19
Bushing	200	7800	0.3

The mechanical parameters are provided in Table 1. The geometric dimensions are shown in Table 2. By applying a uniformly distributed load P_i=15 MPa on the inner wall and crustal stress P_3=20 MPa, the radial stress, circumferential stress, and radial displacement can be calculated.

Table 2. Geometric parameters of casing cement sheath formation system

r_i	r_1	r_2	r_3
110mm	122mm	165mm	500mm

Fig. 2(a) shows the stresses are distributed along the radius. In an ideal elastic state, the inner wall primarily experiences radial pressure, which leads to internal compression. The radial stress is higher near the inner wall due to the radial contact force. The Poisson effect causes radial compression and tensile deformation in the circumferential direction, resulting in greater circumferential stress at the outer diameter of the sheath. Fig. 2(b) illustrates

the relationship between radial displacement and radius. At the inner boundary, the outward radial stress results in an outward movement of the inner boundary. Conversely, at the outer boundary, inward constraints lead to negative radial displacement due to the inward movement under pressure. This demonstrates that the cement sheath experiences overall compression under radial pressure.

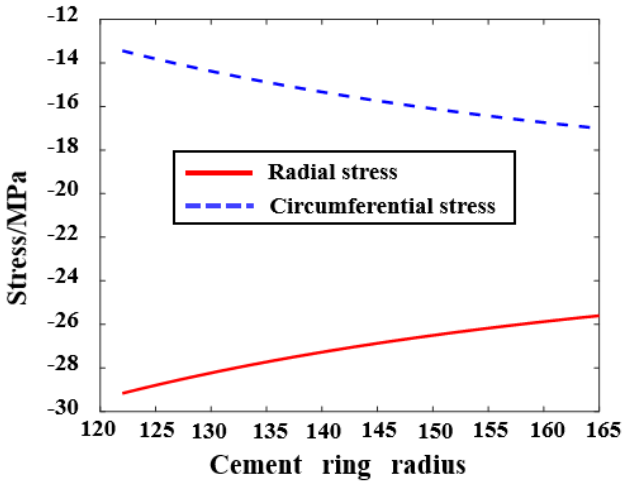

(a) Stress Distribution

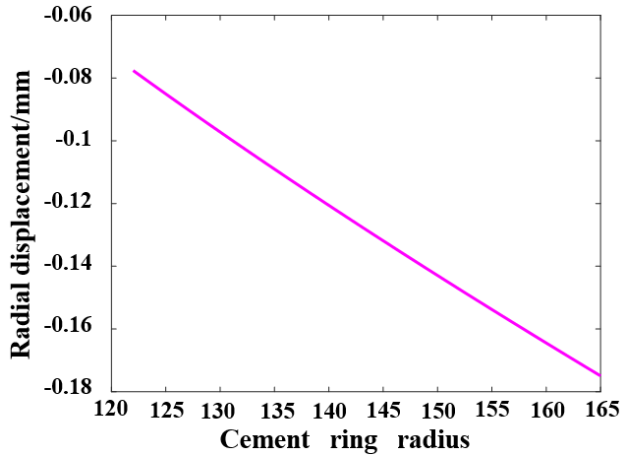

(b) Radial Displacement Distribution

Fig. 2. Analysis Model of Cement Ring

4. Result Analysis and Discussion

4.1 Model validation

A finite element model was established to verify the accuracy of the analytical model, as shown in Fig. 3. The model consisted of a square formation with a side length of 500 mm. The inner radius was r_i =110 mm, the outer radius was r_1 =122 mm, and the outer radius of the cement sheath was r_2 =165 mm. Consequently, the casing wall thickness was 24 mm, whereas the cement sheath wall thickness was 43 mm. Material parameters are listed in Table 1.

Radial stress and displacement distributions were computed, as shown in Fig. 4. The radial stress and displacement values were extracted as numerical solutions for the elastic deformation stage. These results were compared with finite element numerical solutions to verify the accuracy of theoretical derivation and numerical models.

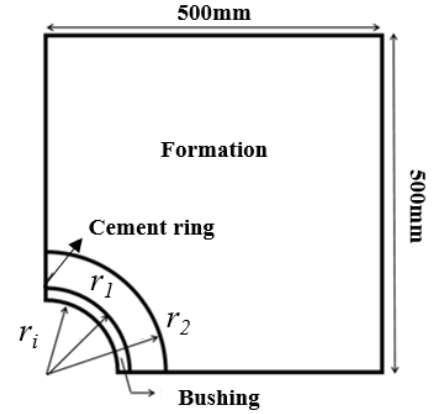

(a) Geometric Model

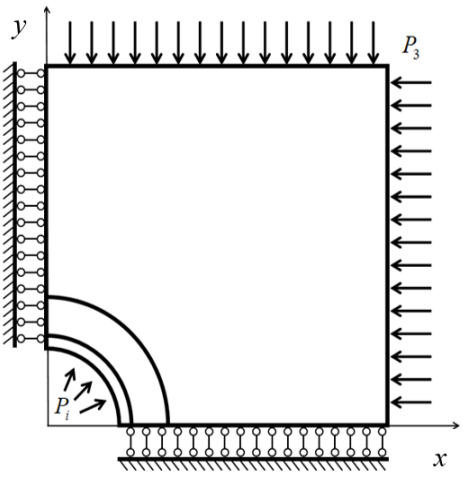

(b) Boundary Conditions and Loads

Fig. 3. 2D Finite Element Model of Casing Cement Sheath

By comparing the mechanical response analytical model and numerical solution, as shown in Fig. 5, the analysis revealed that the stress and displacement distributions along the radius were consistent in terms of numerical values and upward or downward trends, thereby demonstrating the accuracy of the theoretical derivation.

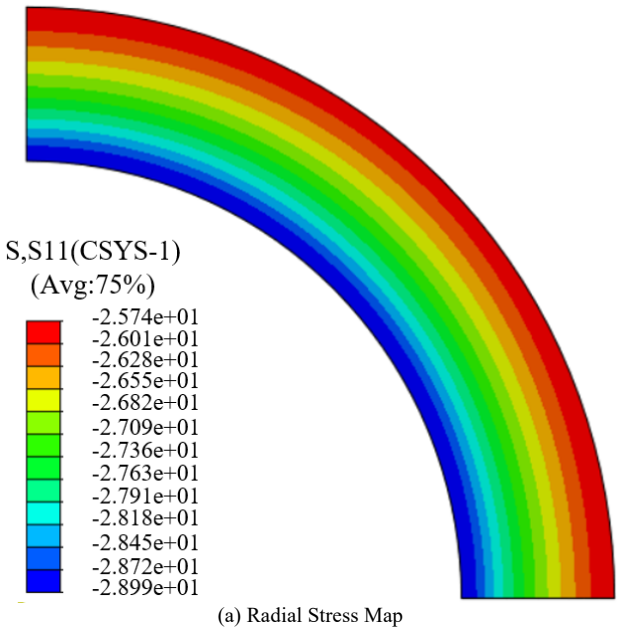

(a) Radial Stress Map

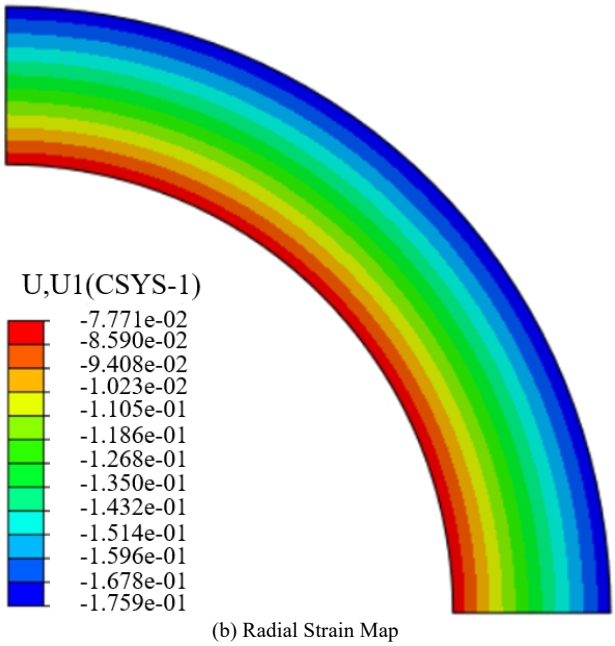

(b) Radial Strain Map

Fig. 4. Elastic Deformation of Cement Sheath

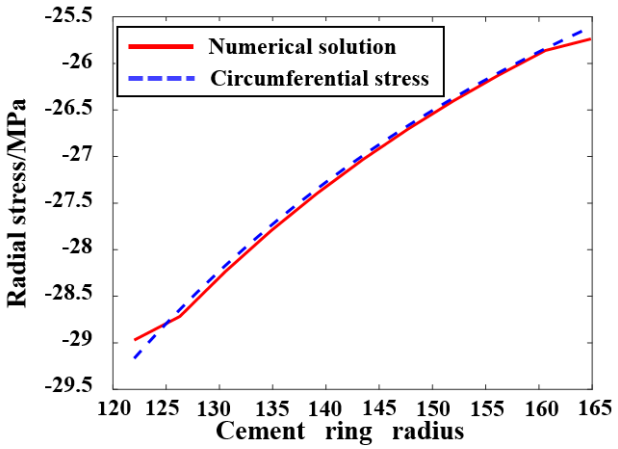

(a) Stress

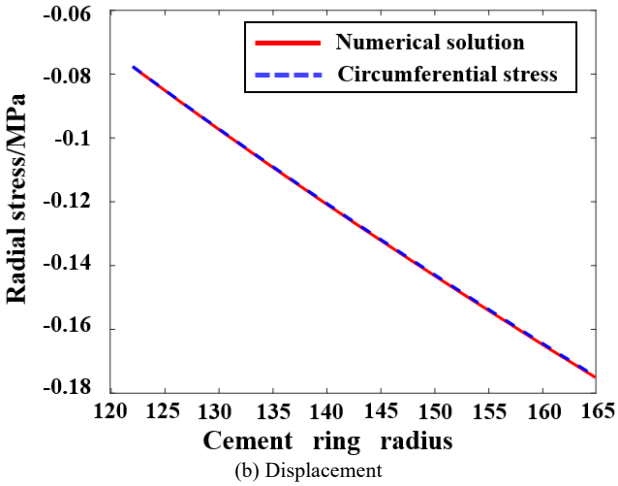

(b) Displacement

Fig. 5. Radial Distribution of Stress and Displacement

4.2 Parameter influence law

This section further compares the effects of various parameters on the stress field and displacement field during the elastic deformation phase.

4.2.1. Elastic modulus of cement sheath

This study investigates critical radial positions within the cement sheath at r = 122 mm, 132 mm, 142 mm, 152 mm, and 162 mm. The radial stress and displacement at these positions are calculated as the elastic modulus is increased in ten equal increments, ranging from 10 GPa to 60 GPa.

Fig. 6(a) illustrates that the relationship was linear; the effect was more pronounced in the inner regions and less significant at larger radii. The impact of the elastic modulus on radial stress was more pronounced in the inner regions and becomes less significant at larger radii. When the elastic modulus exceeded 40 GPa, its effect on radial stress stabilizes, as the cement sheath material became sufficiently rigid and resistant to deformation. Consequently, further increases in elastic modulus resulted in minimal changes in radial stress. Fig. 6(b) illustrates that radial displacement decreased with increasing elastic modulus, approaching zero, as the deformation diminished.

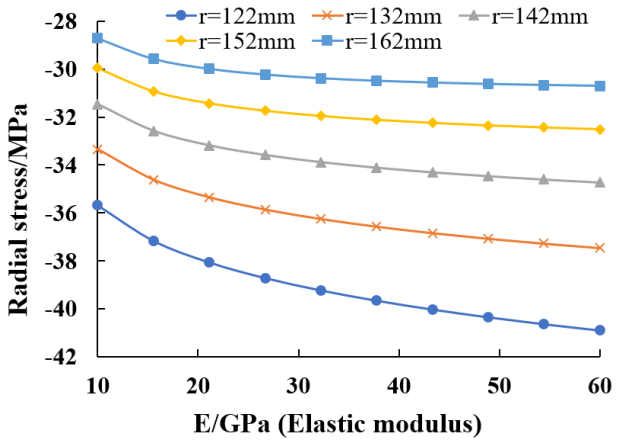

(a) Radial Stress

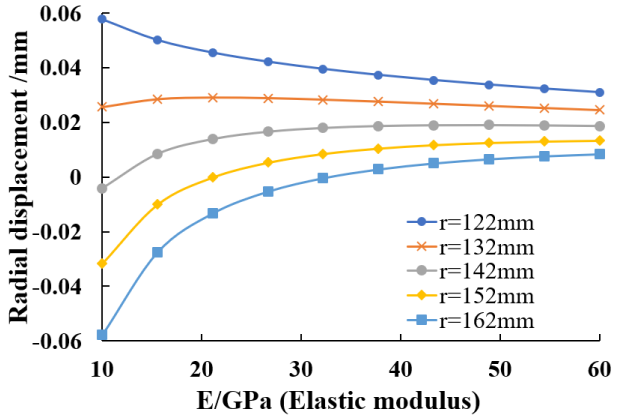

(b) Radial Displacement

Fig. 6. Effect of Elastic Modulus

4.2.2. Poisson's ratio of cement sheath

The Poisson's ratio was increased in ten equal increments, ranging from 0.1 to 0.3, and the resultant changes in stress and displacement were calculated, as depicted in Fig. 7. Fig. 7(a) reveals that variations in Poisson's ratio induced only minor alterations in radial stress, thereby indicating a limited influence of Poisson's ratio on stress distribution. Fig. 7(b) illustrates that Poisson's ratio exerted a minimal effect on radial displacement, manifesting as a slight augmentation at the inner wall and a marginal reduction at the outer wall. Notably, the relative displacement between these two positions remained almost unaltered. This observation agreed with the marginal impact as shown in Fig. 7(a).

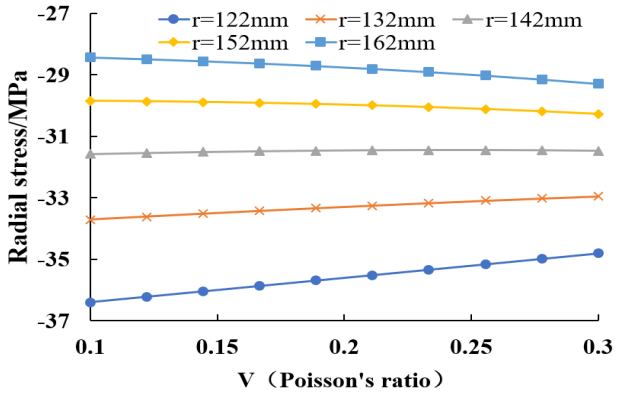

(a) Radial Stress

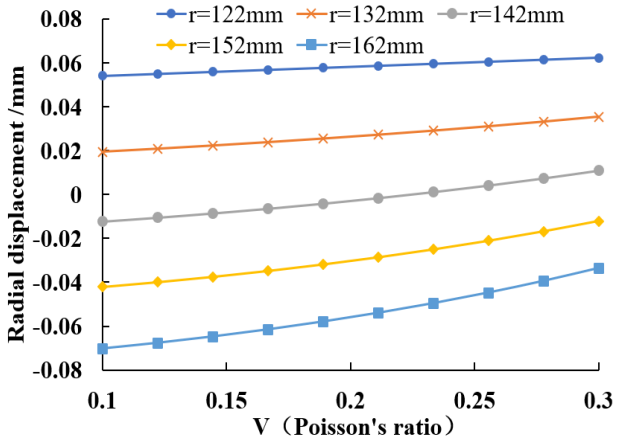

(b) Radial Displacement

Fig. 7. Effect of Poisson's Ratio

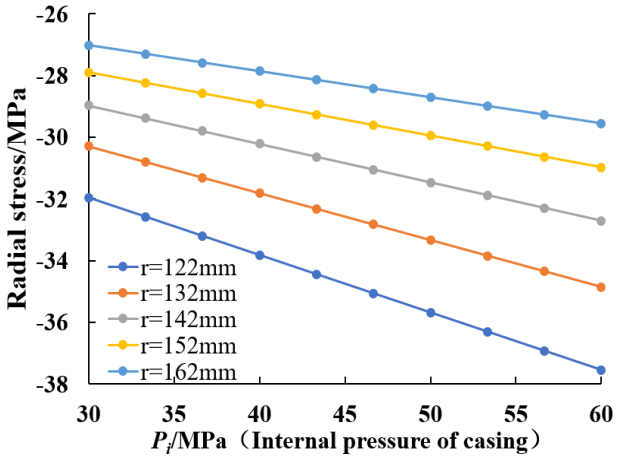

(a) Radial Stress

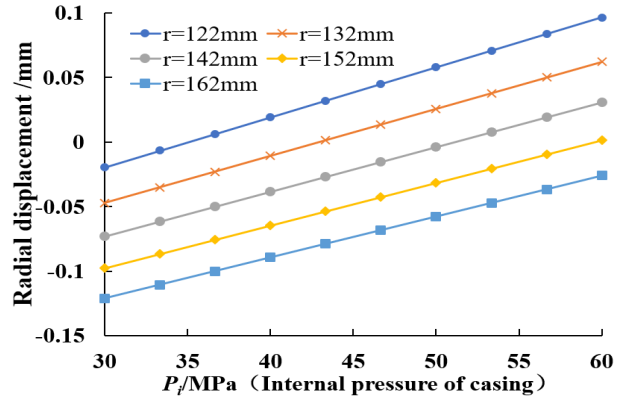

(b) Radial Displacement

Fig. 8. Effect of Casing Pressure

4.2.3. Internal pressure of casing

The casing internal pressure was increased in ten equal increments from 30 MPa to 60 MPa, and the corresponding changes in stress and displacement were calculated, as shown in Fig. 8. Fig. 8(a) illustrates that the radial stress with the cement sheath increased with internal pressure. Fig. 8(b) reveals that radial displacement initially decreased and subsequently rose, transitioning from negative to positive. Initially, an elevation in internal pressure induced radial compression of the cement sheath radially. However, when the internal pressure exceeded a specific threshold, the cement sheath commenced radial expansion, resulting in augmented radial displacement. Consequently, beyond this threshold, the cement sheath underwent a transition from a state of radial compression to expansion, ultimately yielding tensile state in the circumferential direction.

5. Conclusions

To investigate the stress and displacement fields within the cement sheath during elastic deformation and their influencing factors, this study developed an analytical model using MATLAB. This model examined the effects of the cement sheath's elastic modulus, Poisson's ratio, and casing internal pressure on the stress and displacement fields. The following conclusions could be drawn:

(1) The cement sheath as a whole undergoes compression under radial pressure.

(2) The elastic modulus of the cement sheath has a slight effect on radial stress distribution in regions of large radius but significantly affects the inner wall region.

(3) Poisson's ratio does not notably affect radial stress but slightly influences radial displacement, increasing at the inner wall and decreasing at the outer wall.

(4) Radial stress increases with internal casing pressure, whereas radial displacement initially decreases and then increases, transitioning from negative to positive.

This study developed the analytical model for the mechanical response of the cement sheath. It evaluates the influence of various factors on the cement sheath during the cementing process and provides insights for ensuring its integrity. Future work will aim to further refining this model to enhance the understanding of the cement sheath's behavior.

Acknowledgements

This work was supported by the National Key Research and Development Program of China (No. 2019YFC1509204) and the Independent Innovation Research Program of China University of Petroleum (East China) (No.27RA2215005).

References

[1] R. E. Zinkhan and R. J. Goodwin, "Burst resistance of pipe cemented into the earth," *J. Petrol. Technol.*, vol. 14, no. 9, pp. 1033-1040, Sept. 1962.

[2] W. Chu, J. Shen, Y. Yang, Y. Li, and D. Gao, "Calculation of micro-annulus size in casing cement sheath-formation system under continuous internal casing pressure change," *Petrol. Explor. Dev.*, vol. 42, no. 3, pp. 414-421, Jun. 2015.

[3] R. Gholami, B. Aadnoy, and N. Fakhari "A thermo-poroelastic analytical approach to evaluate cement sheath integrity in deep vertical wells," *J. Petrol. Sci. Eng.*, vol. 147, pp. 536-546, Nov. 2016.

[4] G. Shu, *et al.*, "Experimental study on the failure mechanism of cement sheath in gas storage injection and production wells," *Drill. Flu. Com. Flu.*, vol. 37, no. 4, pp. 507-511, Apr. 2020.

[5] A. J. De and S. Sangesland, "Cement sheath failure mechanisms: numerical estimates to design for long-term well integrity," *J. Petrol. Sci. Eng.*, vol. 147, pp. 682-698, Nov. 2016.

[6] K. Deng, *et al.*, "Study on the effect of interface failure between casing and cement sheath on casing stress under non-uniform in-situ stress," *Appl. Math. Model*, vol. 91, pp. 632-652, Mar. 2021.

[7] H. Zhang, W. Wu, and X. Song, "Improved cement sheath thickness measurement and its application in cement sheath variation monitoring," *J. Petrol. Sci. Eng.*, vol. 233, pp. 212-515, Feb. 2024.

[8] X. L. Guo, *et al*., "Influence of tough materials on the integrity of cement sheath interface in shale gas fracturing wells," (in China), *Surf. Tech*., vol. 51, no. 12, pp. 232-242, Dec. 2022.

[9] N. T. Zhou, K. H. Deng, X. P. Chen, Y. H. Lin, K. Yan, and Z. Q. Mei, "Mechanism and control measures of cement ring seal integrity failure under CCUS geological storage," (in China), *Sci. Tech. Eng.*, vol. 23, no. 36, pp. 15448-15455, Dec. 2023.

[10] L. Zhang, H. L. Liu, H. Lin, P. H. Dong, and Y. C. Chen, "A fixed far-field normal displacement elastic-plastic stress solution for cement ring," (in China), *Unconv. Oil & Gas*, vol. 9, no. 4, pp. 107-113, Apr. 2022.

[11] X. G. Wang, Y. X. Wu, S. P. Li, Y. H. Tou, H. Yu, and T. J. Lin, "Analysis of the influence of horizontal well cementing quality on casing deformation," (in China), *Petro. Mach.*, vol. 51, no. 10, pp. 136-143, Oct. 2023.

[12] R. Gholami, V. Rasouli, B. Aadnoy, and M. Mohammadnejad, "Geomechanical and numerical studies of casing damages in a reservoir with solid production," *Rock Mech. Rock Eng.*, vol. 49, pp. 1441-1460, Sept. 2015.

[13] E. R. Ugarte, D. Tetteh, and S. Salehi, "Experimental studies of well integrity in cementing during underground hydrogen storage," *Int. J. Hydrogen Energy*, vol. 51, pp. 473-488, Jan. 2024.

[14] A. Salimi, A.H. Beni, and M. Bazvand, "Evaluation of a water-based spacer fluid with additives for mud removal in well cementing operations," *Heliyon*, vol. 10, no. 4, Feb. 2024.

[15] S. Kumar, A. Bera, and S. N. Shah, "Potential applications of nanomaterials in oil and gas well cementing: current status, challenges and prospects," *J. Petrol. Sci. Eng.*, vol. 213, Jun. 2022, Art. no.110395.

[16] S. Ahmed, H. Patel, and S. Salehi, "Effects of wait on cement, setting depth, pipe material, and pressure on performance of liner cement," *J. Petrol. Sci. Eng.*, vol. 196, Jan. 2021, Art. no.108008.

[17] Z. G. Zheng, K. H. Deng, Y. X. Wu, Z. W. Lin, and Y. H. Lin, "Experimental evaluation of cement sheath integrity during unconventional oil and gas well fracturing process," (in China), *J. Southwest Petro. Univ.*, vol. 45, no. 4, pp. 121-132, Apr. 2023.